BRNO UNIVERSITY OF TECHNOLOGY
VYSOKÉ UČENÍ TECHNICKÉ V BRNĚ

FACULTY OF ELECTRICAL ENGINEERING AND COMMUNICATION
FAKULTA ELEKTROTECHNIKY
A KOMUNIKAČNÍCH TECHNOLOGIÍ

DEPARTMENT OF CONTROL AND INSTRUMENTATION
ÚSTAV AUTOMATIZACE A MĚŘICÍ TECHNIKY

HIGH-RESOLUTION MULTISPECTRAL 3D SCANNING AND ITS MEDICAL APPLICATIONS
MULTISPEKTRÁLNÍ 3D SKENOVÁNÍ S VYSOKÝM ROZLIŠENÍM A JEHO APLIKACE V MEDICÍNĚ

DOCTORAL THESIS
DIZERTAČNÍ PRÁCE

AUTHOR — Ing. Adam Chromý
AUTOR PRÁCE

SUPERVISOR — prof. Ing. Luděk Žalud, Ph.D.
ŠKOLITEL

BRNO 2017

CONTENTS

1 INTRODUCTION

During last years, availability of thermal imagers moved from expensive, bulky and cumbersome systems to affordable and practical solutions [11]. Due to such rapid progress, the thermal imaging slowly penetrates to everyday practice also in areas, where it was recently used in research studies only.

An exemplary case of such an area is medicine. The digital medical thermal imaging (DMTI), a modality of medical imaging for monitoring the surface of the skin temperature, is evolving over the last 50 years, however, this technology is still considered as *qualitative* tool, enabling to distinguish between physiological and non-physiological states of body, but without ability to *quantify* them.

Another rapidly progressing technology is 3D scanning. 3D surface models are more and more used in situations, where state of any object must be preserved in permanent, time-invariant state. In this case, colour-covered 3D models seems to be the best modality [12]. Also the domain of object cloning is rapidly growing today. There are lots of 3D printers available on the market now, and each of them requires tool for building 3D model to be printed [13]. Finally, computer 3D models are, due to its plasticity, becoming more and more used for visualization of objects, which are visible, but its important details are too tiny, that it is necessary to enlarge them plastically [3]. And exactly these applications have the potential to be used also in healthcare.

If these two modern and progressive technologies were combined, we could get even more new information than if they were applied separately. Such data fusion will bring new benefits, addressing long-term problem of *medical quantification*, that permeates across the entire healthcare system and is still not reliably solved. With too inaccurate, insensitive or subjective evaluation methods is struggling, for example, dermatology or physiotherapy.

In this thesis, the author is developing new multispectral 3D surface scanning system RoScan, combining thermal imagery with colour 3D surface scanning in novel way, which is extending DMTI with the ability of *quantification*, but also brings several other advances beyond the current state of the art.

The RoScan is multi-purpose device, having its application in many different sectors, however, the research is mainly focused to medicine, which offers many opportunities. By this research, author is contributing to making medical quantification in several sectors of medicine more objective.

Although the work focuses mainly on medical problems, it does not mean that it is useful only for them. It is also usable, for example, in mechanical engineering, civil engineering, electrical engineering, museums or restoration.

2 STATE OF THE ART

In this chapter, only the brief summary of state of the art is presented. Current methods and their characteristics can be found in the full text of thesis.

The first part summarizes the current state of 3D thermal imaging applied in medicine, what is directly the area of this thesis (section 2.1).

According to findings of this survey, the current solutions of 3D thermography suffer with several drawbacks, that are conditioned by the method used. For this reason, in section 2.2, an overview of current available 3D surface scanners was formulated, with focus on their principles, and mainly advantages and disadvantages of these approaches.

In this background research, it was found that the most suitable solution of 3D surface scanning is based on robotic manipulator, so next overview in section 2.3 is devoted to robotic 3D scanning.

Considering the knowledge from these section, the novel multispectral 3D surface scanning system was then developed (chapter 4).

Next sections 2.4 and 2.5 deals with current state of both selected clinical applications, in which the developed device brings advances beyond their state of the art and in which the pilot experiments were taken.

2.1 Medical Applications of 3D Thermal Imaging

Current solutions of 3D thermography are based on stereophotogrammetry, structured-light scanning or infrared depth sensors. As the most suitable for medical quantitative applications seems to be the method using structured-light or stereo structured-light, due to the precision. Methods using stereophotogrammetry or cheap depth cameras (Kinect, ASUS Xtion) are unreliable, respectively inaccurate, so their use in medical applications is not recommended.

All thermal 3D scanning solutions, presented in publications, introduced its principles and showed samples of 3D scans, however, no further clinical applications were found.

Since thermal changes inside the body are usually small and can be hidden in physiological gradients of temperature, according to [14], it is necessary to provide data with many times higher resolution than presently available devices are able to. Such images shall be also big enough to see all the processes in the region.

And this is the important limitation of each mentioned method – the thermal layer has significantly lower resolution than 3D surface model below, what is excluding many potential application. The surfaces with high resolution are also too small, and cannot be combined without important loss of accuracy. This may be also the reason why proposed methods are not used in current practice.

Thus, the method capable of capturing large 3D surface models, where the resolution of 3D surface, color data and thermal data is the same and very high, is still missing.

2.2 High-Resolution 3D Surface Scanning

There any many different 3D surface scanners available on the market, when each one is adapted for the application, which it is primarily intended for. Rather than evaluating each model of 3D scanner, we discuss each available implementation of every module with emphasize on medical application of 3D scanner.

The blocks, which each scanner consists of, are further described in the full text of thesis.

Regarding the potential applications of 3D surface scanning in medicine (chapter 1) and taking into account the required properties resulting from it, we can define, using knowledge of current scanner implementations, how particular modules shall be realized.

Ideal medical 3D surface scanner shall use structured-light scanning or triangulation laser scanning for raw data capturing, due to its accuracy. Sensor motion shall be motorized to be able to automate the process and kinematic chain must be used for precise localization. It should have at least 6 DOF to reach sufficient flexibility. The data shall be stored in form of point-cloud or mesh.

There is no commercial device meeting all the criteria defined above, such flexible and accurate 3D surface scanning system is not available on the market yet. Generally speaking, all the commercially available 3D scanners are compromise between two important abilities: *accuracy* and *flexibility* [15], but for the medical purposes, both accuracy and flexibility is needed.

However, there were found some research experimental setups using robotic manipulator in medical imaging, what is a constitution, that is meeting our criteria for medical 3D surface scanner. Thus, special survey of state of the art related to robotic 3D scanning had been performed and presented in following section.

2.3 Robotic 3D Scanning

From 10 research studies that were found as using robotic manipulator for 3D scanning purposes, just 6 of them were focused on capturing 3D surface models.

Two 3D surface scanning studies were moving with scanned object by robotic manipulator, what is out of question for medical imaging of humans.

Another two of them were using stereophotogrammetry to estimate the spatial data, what is a generally accurate method, but failing in homogeneous areas, which are often present of human body.

The remaining two studies may be considered as applicable to medical 3D surface scanning. The first is using heavy, fast and accurate 3D scanner, while the second is using light, but slow and less accurate laser gauge. For optimal performance, the solution in the middle between these two seems to be the best solution.

2.4 Quantification of Dermatitis

Dermatitis is manifested by many different symptoms (redness, edema, oozing, dryness etc.) and for each of them, a bioengineering method exists. However, this methods are focused on single or few dermatitis manifestations only, not for the disease as a whole.

The overall rating of dermatitis severity provides the scoring systems only, but even the best ones of them are still very subjective, insensitive and providing small resolution.

Bioengineering methods correlate with subjective evaluations of severity or with scoring systems, but they often correlate with each other moderately of poorly. This shows, that many symptoms of dermatitis are individual (e.g. somebody is more crusting but less swelling, etc.).

Symptoms, which were found as expressing more or less the same way at all individuals (hence the most objective) are the increased blood flow and changes of thickness of particular skin layers [16]. Taking into account only measurements of them, it will eliminate the list of potentially reliable methods to Thermal Imaging, FDI, HFUS, OCT and RCM.

The sensitivity of HFUS is sometimes insufficient, what prefers using OCT or RCM. However, the HFUS, OCT and RCM are objective, but interpretation of data requires experienced clinician, what can cause misinterpretations or uncertainties.

The FDI and Thermal Imaging are straightforward and easily interpretable. But the FDI's blood flow is measured only in narrow selection, not in the whole tissue, what can lead to false interpretations. Thermal Imaging is assessing blood flow globally, but it is limited by inability of quantification.

So there remains an unmet need for more definitive and reliable non-invasive assessment technique in dermatology [17].

2.5 Volumetric Measurements of Soft Tissues

The ideal volumetric method for measurements of limb volume should be accurate, repeatable, operator independent, simple to use, inexpensive, fast and allowing selection of arbitrary region of interest. Except the last two capabilities, the Water Displacement Method has all of them, so it is conclusively recommended as a golden standard.

However, although it has many advantages, the impossibility of choosing region of interest is a significant limitation. In many applications, this is indispensable requirement, what force researchers and clinicians to use slow, expensive and cumbersome method: volumetry using MRI or CT, what are devices primarily intended for different purposes.

Capacity of locations equipped by these imaging modalities, which is very limited, excludes frequent repeated measurements of single subject, what makes specific volumetric monitoring impossible.

Also even if using MRI or CT, the selection of region in 3D model is possible, but special markers must be used, which has also their limitations.

So there is still a need of volumetric method, which is comparable with Water Displacement Volumetry, but allowing advanced selection of region of interest.

3 AIM OF THE DOCTORAL THESIS

From current state of the art follows, that the method, which is key for medical quantification using thermal imaging, is still missing. Background research also advised, that the solution could be a method capable of capturing large 3D surface models, where the resolution of 3D surface, colour data and thermal data is the same and very high. Analysing of principles used in today's 3D scanners give us a hint, from which components the method shall be composed from. It was also found, that such device is not currently available. As a reason of this, the 3D scanning system, bringing required capabilities, must be developed on our own, by combination of most suitable components.

Thus, the aims of this thesis can be formulated as follows:

1. The main aim of this thesis is research and development of 3D multispectral surface scanner, bringing advances beyond the current state of the art by being capable of capturing both large and high-accurate surface scans, containing spatial information, colour and temperature. Such device currently does not exist.
2. This device shall be supplied also with software providing sufficient functions to analyse scanned data in terms of spatial measurements and thermal analysis.
3. The accuracy parameters shall be specified and properly verified.
4. The contribution of this device to the problem of medical quantification shall be demonstrated by appropriate experiments, proving the capability of created system to bring advances beyond state of the art in selected clinical applications.

Regarding the knowledge from the state of the art, meeting these points is assumed using robotic manipulator equipped with 2D laser scanner, what is expected as suitable trade-of between two solutions described in state of the art – fast, but heavy, bulky and cumbersome solution using commercial 3D scanner, and lightweight, small, but slow solution using 1D laser gauge. Robotic manipulator will be also equipped with colour and thermal camera in order to reach required multispectrality.

Such system should be verified in practical applications in physiotherapy and dermatology, where should contribute to solve the current issues, outlined in the state of the art.

4 ROSCAN – MULTISPECTRAL ROBOTIC 3D SURFACE SCANNER

RoScan is a multispectral robotic 3D scanning system designed for capturing 3D computer models of surface (Fig. 4.1). Each such model, besides the spatial representation of the object itself, also contains information about the temperature, colour and index of roughness.

Fig. 4.1: Multispectral robotic 3D scanning system RoScan.

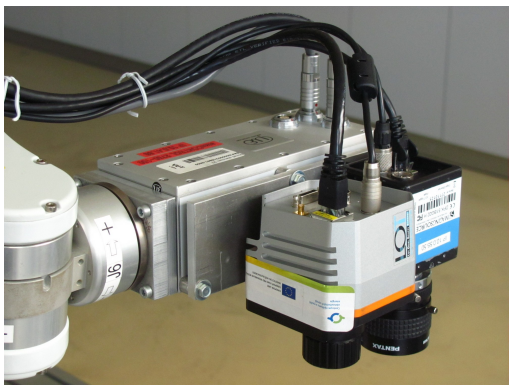

Fig. 4.2: Sensoric head: 2D laser scanner (left), thermal imager (middle) and RGB color camera (right).

In following text, only outline of solution is presented together with its capabilities. Full implementation is described in full text.

4.1 Technical Concept of RoScan

The hardware part of RoScan is composed from the robotic manipulator with sensoric head (Fig. 4.2), equipped with 2D planar laser scanner, RGB colour camera, thermal camera.

In our experimental setup, we use the 6-axis industrial manipulator EPSON C3, which is reaching accuracy of end-point placement $\Delta_M = \pm 0.013$ mm. Besides perfect accuracy, it disposes with fast speed and sufficient operational range.

To gain data for 3D surface generation, we use planar proximity 2D laser scanner MicroEpsilon ScanCONTROL2750-100. Since it is based on triangulation principle, it deals with high accuracy of $\Delta_S = \pm 0.027$ mm .

Sensoric head is also equipped with LWIR thermal camera Xenics GOBI1954 with resolution 384×288 pixels, pixel pitch 25 µm and spectral response fo wavelength range $8 - 14$ µm. There is also a colour camera ImagingSource DFK 51BG02.H with resolution 1600×1200 pixels and $1/1.8''$ Sony CCD chip.

This sensor combination has been tested and assessed as suitable for body scanning in high resolution, but it is important to say, that entire solution of RoScan system is independent on used components. User can easily change any device with another.

Workplace with RoScan is shown in Fig. 4.3. Using of manipulator with at least 6 degrees of freedom empowers flexibility to the system and because of this, it is possible to measure all parts of human body (Fig. 4.4).

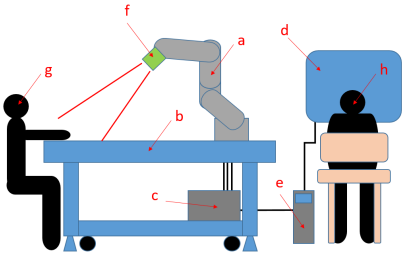

Fig. 4.3: Overview of RoScan system workplace.

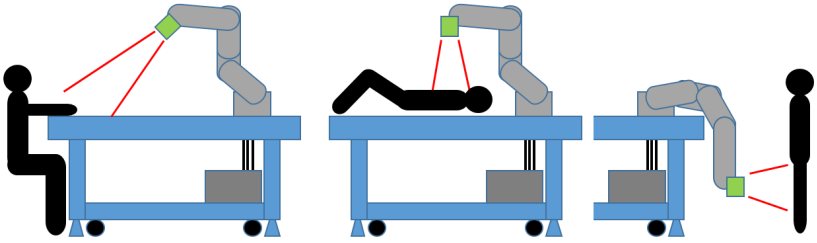

Fig. 4.4: Flexibility of use – some of possible configurations of robot during scanning.

The core of the solution lies in the software, running on the main computer, which performs control of the scanning process and serves also as computational unit for processing the data from sensors to the form of multi-layered 3D model. This core software is outlined in the Fig. 4.5 with blue dashed line.

Scanning process pipeline begins with user input to **Trajectory Definition** module. Desired path of motion can be described by simple scripting language allowing definition of required trajectory using geometric primitives like points, lines or arcs.

Such recipe ($\mathbf{C}_{0,\mathrm{w}}$) is then passed to **Trajectory Compilation**, which converts human-readable trajectory description $\mathbf{C}_{0,\mathrm{w}}$ to the machine-readable form $\mathbf{P}_{\mathrm{M,w}}$, what is a sequence of 6-DOF[1] points to be visited by manipulator using point-to-point motion (PTP).

Module **Executing Predefined Trajectory and Sensor Sampling** sequentially processes the given list of points $\mathbf{P}_{\mathrm{M,w}}$. At each item, the module sets end-point of manipulator to the pose $\mathbf{p}_{\mathrm{M,w}}$ over its *C# Driver* and waits for the confirmation. Reaching the desired pose is confirmed by sending true pose of robot $\mathbf{p}_{\mathrm{M,r}}$ back to the software. At this time, the module asks for data from 2D laser scanner ($\mathbf{d}_{\mathrm{L}}$ and $\mathbf{I}_{\mathrm{R}}$) and/or for data from colour camera $\mathbf{I}_{\mathrm{C}}$ and thermal imager $\mathbf{I}_{\mathrm{T}}$ (also through their C# drivers). Which data shall be collected in each pose is also part of trajectory definition $\mathbf{P}_{\mathrm{M,w}}$. The author is aware, that this solution may slow down the entire process, because only one component is active at each time, but this disadvantage is redeemed by benefits, since time synchronization of captured data is then simple and secure, even if the TCP/IP over Ethernet is naturally a non-deterministic communication.

[1]Six degrees of freedom. In context of points, it means that point in space is described with 6 coordinates: 3 Cartesian coordinates to define a spatial location and 3 rotational coordinates in RPY notation to define the orientation of object in this location (e.g. manipulator end-point pose, camera direction of view, etc.).

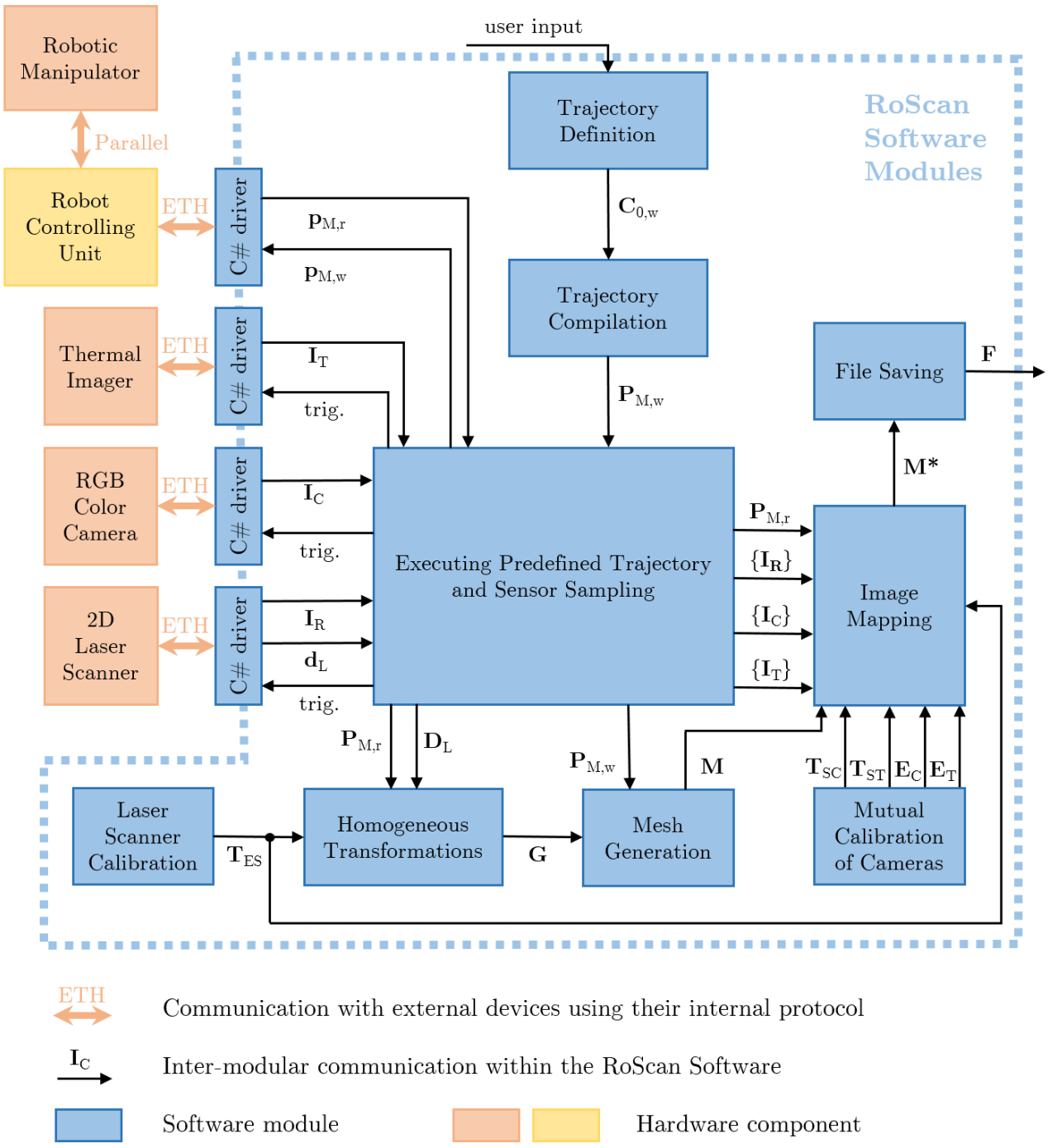

Fig. 4.5: Overview block diagram showing essential modules of system RoScan.

Captured profiles $\mathbf{D}_L$ are then passed to the module of **Homogeneous Transformations**, which transforms measured distance profiles in coordinate system L to the world coordinate system 0. Result of this process is $\mathbf{G}$, the structure similar to the point-cloud.

Entire transformation is given as sequence of essential transformations between neighbour

coordinate systems:

$$\mathbf{p}_0^{\mathrm{H}} = \mathbf{H}_{0\mathrm{M}}\mathbf{H}_{\mathrm{ME}}\mathbf{H}_{\mathrm{ES}}\mathbf{H}_{\mathrm{SL}}\mathbf{p}_{\mathrm{L}}^{\mathrm{H}} \tag{4.1}$$

where $\mathbf{p}_0^{\mathrm{H}}$ is point in three-dimensional coordinate system 0 expressed using homogeneous coordinates, $\mathbf{p}_{\mathrm{L}}^{\mathrm{H}}$ is such a point in system L, $\mathbf{H}_{\mathrm{AB}}$ is homogeneous transformation matrix performing transformation from B to A, 0 are world axes, M are manipulator axes, E are manipulator's end-point axes, S are laser scanner axes and L are laser emitter axes.

Partial transformations are derived in full text, what leads to equations:

$$\begin{aligned}
\mathbf{p}_{\mathrm{L}}^{\mathrm{H}} &= \begin{bmatrix} 0 & 0 & d_{\mathrm{L,i}} & 1 \end{bmatrix}^T && (4.2)\\
\mathbf{H}_{\mathrm{SL}} &= \mathbf{Rot}_y\left(\alpha_{\mathrm{L,i}}\right) && (4.3)\\
\mathbf{H}_{\mathrm{ES}} &= \mathbf{Trans}\left(x_t, y_t, z_t\right)\mathbf{Rot}_z\left(u_t\right)\mathbf{Rot}_y\left(v_t\right)\mathbf{Rot}_x\left(w_t\right) && (4.4)\\
\mathbf{H}_{\mathrm{ME}} &= \mathbf{Trans}\left(x, y, z\right)\mathbf{Rot}_z\left(u\right)\mathbf{Rot}_y\left(v\right)\mathbf{Rot}_x\left(w\right) && (4.5)\\
\mathbf{T}_{\mathrm{ES}} &= \begin{bmatrix} x_t & y_t & z_t & u_t & v_t & w_t \end{bmatrix}^T && (4.6)\\
\mathbf{p}_{\mathrm{M,r}} &= \begin{bmatrix} x & y & z & u & v & w \end{bmatrix}^T && (4.7)
\end{aligned}$$

where $d_{\mathrm{L,i}}$ is distance of point from laser emitter. This value is returned by laser scanner, together with measuring angle $\alpha_{\mathrm{L,i}}$. Matrix $\mathbf{Trans}\left(x, y, z\right)$ is standard homogeneous translational matrix, $\mathbf{Rot}_a\left(b\right)$ in standard homogeneous matrix defining rotation about axis a by angle b, $\mathbf{T}_{\mathrm{ES}}$ is transformation describing position of laser scanner on end-point and $\mathbf{p}_{\mathrm{M,r}}$ is pose of manipulator when measuring distance relevant to evaluated point.

In our case, system 0 is identical with system M. If it is not, another matrix similar to $\mathbf{H}_{\mathrm{ME}}$ can be used.

Since the transformation process of single point is not dependent on the others, the module is not waiting until all data are captured, but starts with conversion immediately with first available rows of $\mathbf{D}_{\mathrm{L}}$ and $\mathbf{P}_{\mathrm{M,r}}$. This processing pipelining is used also in following Mesh Generation block, what allows faster throughput and empowers the possibility of having 3D shaded model $\mathbf{M}$ already computed at the end of scanning.

Because mesh representation of 3D data is more illustrative then point-clouds, the **Mesh Generation** module was developed, which processes $\mathbf{G}$ to the form of shaded 3D model of surface ($\mathbf{M}$). In the RoScan system, two different methods are used, selectable in main settings of the system.

First is a Delaunay Triangulation [18], which is usable for totally unorganized sets of points. Its limitation is, that density of points must be very high, otherwise the surface can be wrongly interpreted. It is also computationally demanding, what makes it significantly slow. From these reasons, this method is used rarely, just in cases, when second method fails.

The second method is used as default, and even it is very simple, in most occasions works well. The method is based on polyhedral terrain model [19]. It uses not only pure point-cloud

data, but also additional information about order, in which they were scanned, and which point of scanning trajectory they were scanned from.

If object and trajectory are simple, each of its particular small areas of surface can be considered as terrain map projected into the plane perpendicular to direction where scanner looks at. And in this view, the nearest neighbours on the surface are points, which were scanned just in sequence, one after another, as same as points, which were scanned with same ordering number in two subsequently captured profiles.

From these two findings about neighbours, we can compose scanned points to triangles. This process and triangulation equations are further described in full text.

Such model is further processed in **Image Mapping** block, where several additional layers are added. In resulting multi-layered model $\mathbf{M}^*$, each point contains, in addition to its position itself, also the temperature, colour and roughness index. These values are computed by projecting sequences $\{\mathbf{I}_\mathrm{C}\}$, $\{\mathbf{I}_\mathrm{T}\}$ and $\{\mathbf{I}_\mathrm{R}\}$ on the 3D surface.

The main idea of image mapping algorithm is in tracing of rays [20] from each single point of scanned 3D model to camera origin. Using pinhole camera model, we are tracking each such ray and we are examining where it strikes the plane of light-sensing chip. This location is expressed with subpixel resolution, and appropriate value belonging to examined point is given by interpolating 4 nearest pixel values. During the ray tracing, also intersection with model is examined, in order to exclude points, which are not visible in the image due to masking by part of the model, which is closer to camera.

Because the ray tracing itself is very computationally demanding procedure, we are gradually eliminating vertices, which are clearly out of the view. For each vertex of 3D model $\mathbf{M}$, following steps are taken:

1. Checking, if the ray pointing from camera origin to examined point intersects the plane, in which the light-sensing chip lays. If there is an intersection point, we are continuing the algorithm. Otherwise, we skip following steps and continue with step 1 for next point of 3D model.
2. Checking, if intersection point lays within image rectangle, i.e. if ray strikes the chip or not.
3. Checking, if ray intersects 3D model or not, i.e. if point is *directly* visible. The easiest way to find the intersection is to check, if ray intersects *any* of triangles, which 3D model composes from. For checking ray-triangle intersection, the algorithm of [21] is used. When single ray-triangle intersection is found, the iterating is stopped immediately and we skip. For optimization of checking all the triangles for intersection, the model is kept in hierarchical Octree structure [22], allowing significantly decrease number of triangles to be tested for intersection. This structure is described more deeply in the full text.
4. Mapping of value to point using interpolation of 4 neighbouring pixels. When single point is simultaneously visible on more images, the resulting value is given as average of values acquired from each image.

These algorithms, even if developed for RoScan, are applicable to *general* digital 3D model of object and *general* 2D images.

Finally, the model $\mathbf{M}^*$ is stored in **File Saving** module to the file $\mathbf{F}$ in author's own format for further analyzing.

Format of the file was designed with aim to be flexible and easily extensible for future abilities. More accent is also put on the backward-compatibility. There is a XML structured file, which consists from several blocks. There are 4 required blocks, sufficient for building basic 3D model $\mathbf{M}$: metadata (time of file creation, author, etc.), vertices (serialized vector of vertices, i.e. spatial points), indices (serialized vector of point triplets, connecting vertices to triangles) and trajectory (serialized vector $\mathbf{P}_{\mathrm{M,r}}$, representing real trajectory).

Other blocks are optional and can be even further extended during future development of system. The advantage is, that structure of file can be modified by adding new blocks and it will be still readable in older versions, disadvantage is large size, but it is solved by binary serialization followed by Base64 encoding [23], which is applied to large data blocks, like vertices and indices.

To eliminate unwanted 3D model distortions and errors in mapping of colour and thermal information on the surface, two calibration procedures were developed.

The projection of captured points to the world coordinate system is significantly influenced by $\mathbf{T}_{\mathrm{ES}}$, the transformation defining position of laser scanner relatively to the end-point of robotic manipulator. Since inaccuracies in $\mathbf{T}_{\mathrm{ES}}$ causes several distortions of object, it is necessary to know this transformation very accurately. Evaluation of $\mathbf{T}_{\mathrm{ES}}$ is a purpose of **Laser Scanner Calibration** method.

Since the method is relatively complex, it is not possible to describe it in few lines here. Basically, it is based on exploring differences between same scene captured from two directions (Fig. 4.6). The difference $\mathbf{\Delta}_{\mathrm{ES}}$ between true value and used value of $\mathbf{T}_{\mathrm{ES}}$ is estimated from distortions, which are presented in first scan differently than on the second, or on both but with different sign (Fig. 4.7).

Since this analytic approach requires several preconditions to be fulfilled and they are usually not, the calibration constants are evaluated only roughly using these algorithms. As a reason of this, they are finely adjusted in second step, which is based in numeric solution minimizing the error function.

Similarly, the correct mapping of 2D images on the surface of 3D model is subject to accurate knowledge of cameras position relatively to the laser scanner ($\mathbf{T}_{\mathrm{SC}}$ and $\mathbf{T}_{\mathrm{ST}}$) and their intrinsic parameters ($\mathbf{E}_{\mathrm{C}}$ and $\mathbf{E}_{\mathrm{T}}$). With evaluation of these parameters deals **Mutual Calibration of Cameras**.

The calibration pattern must be visible on all sensors and shall have significant landmark

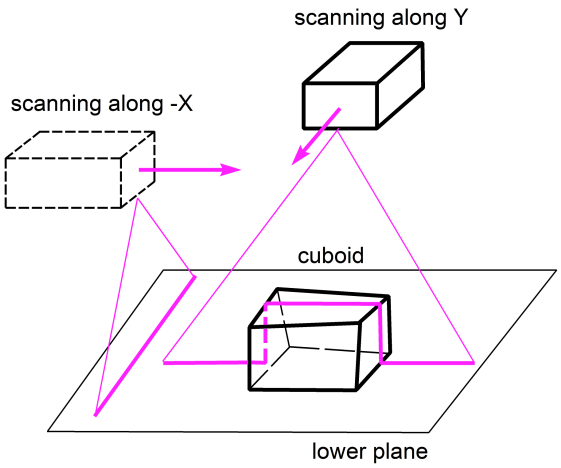

Fig. 4.6: Illustrating basic calibration principle - scanning same scene from two directions.

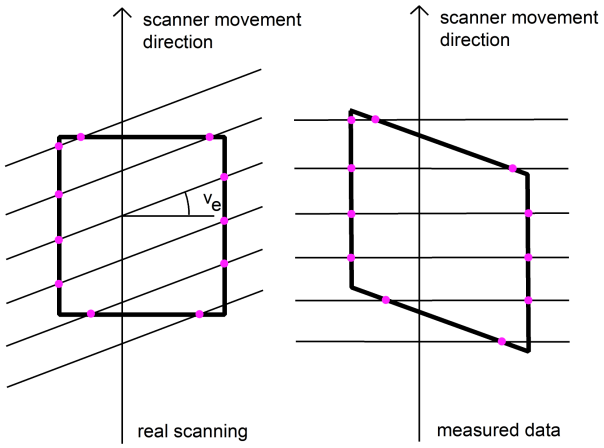

Fig. 4.7: Example of distortion: influence of unknown pitch rotation on object in horizontal projection.

features, clearly visible at images from each sensor. As a result of this, it is made as 4x4 matrix of square holes drilled in the solid square of side 52.5 mm, made from one-sided PCB plate (Fig. 4.8).

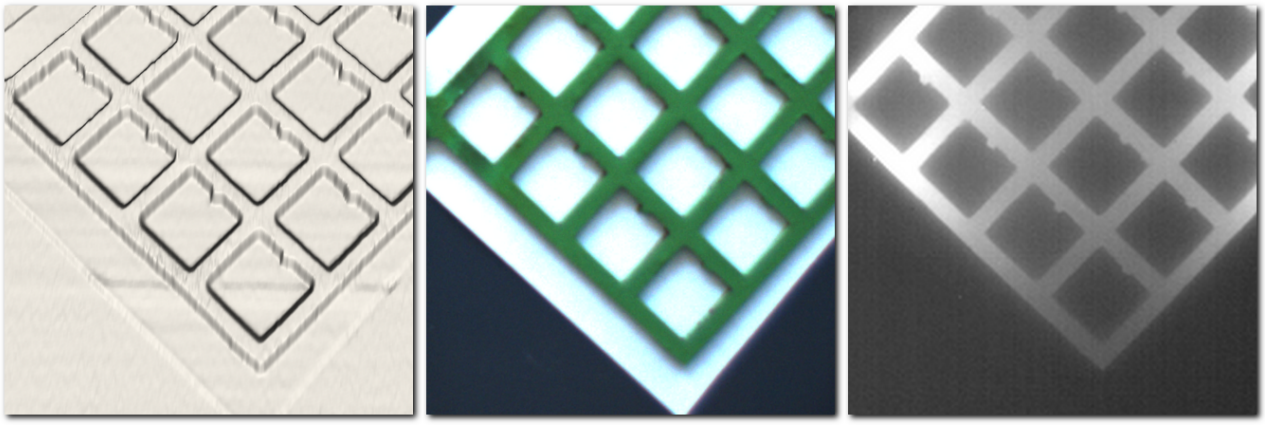

Fig. 4.8: Visibility of calibration pattern and its landmarks on 3D scan (left), color camera (middle) and thermal imager (right).

Using RoScan, the calibration pattern was scanned 20 times without moving with it. Resulting 3D models were then averaged in order to avoid uncertainty of type A. Semi-automated procedure provides 3D coordinates of all 64 reference points at calibration pattern. It is based in edge detection using Canny detector [24], then getting 4 lines approximating square hole edges using Hough transform and then getting 4 corners as intersection points of these lines. The corner detection is not used, because drilled corners are rounded.

Following calibration procedure is then performed for each sensor separately. It consists of several steps, when each item of this list is more deeply described in the full text.

1. **Data Capturing** – Several images of calibration pattern are captured from arbitrary points of view, but from as much as possible different poses. The larger number of images can lead to more accurate solution.
2. **Extracting Corners** – Using same semi-automated algorithm as in reference object, the all corner points of all inner rectangles are extracted from all captured images.
3. **Camera Calibration** – Coordinates of extracted points (2D) are provided to Camera Calibration Toolbox for Matlab [25], together with 3D points extracted from reference 3D scan. Using Zhengyou Zhang's setup, the toolbox computes intrinsic parameters of camera ($\mathbf{E}_\mathrm{C}$ resp. $\mathbf{E}_\mathrm{T}$), and extrinsic parameters $\mathbf{X_i}$ for each captured image.
4. **Evaluating Mutual Transformation** – Outputted extrinsic parameters of images are further processed in order to compute transformations $\mathbf{T_{SC}}$ and $\mathbf{T_{ST}}$. Because manipulator pose is known, we can estimate the transformation from this knowledge and extrinsic parameters.

Note, that this solution is useful not only for this particular setup, since it can be generalized for any number of sensors and arbitrary 3D scanner setups.

4.2 Software tool RoScan Analyzer

Multispectral 3D surface models created by RoScan and stored in form of **F** can be displayed in visualizing tool RoScan Analyzer (Fig. 4.9 and 4.10).

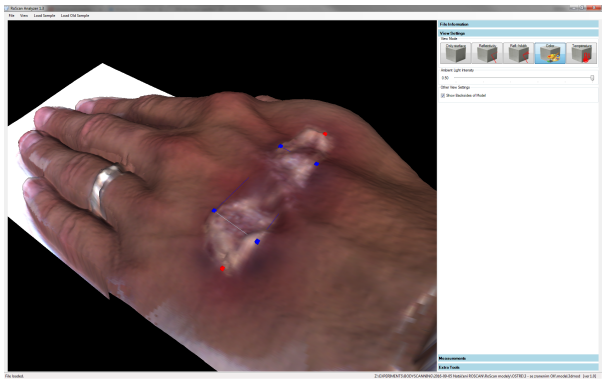

Fig. 4.9: Detail of 3D model of hand with presumed burn shown in the true colour view with selection markers applied.

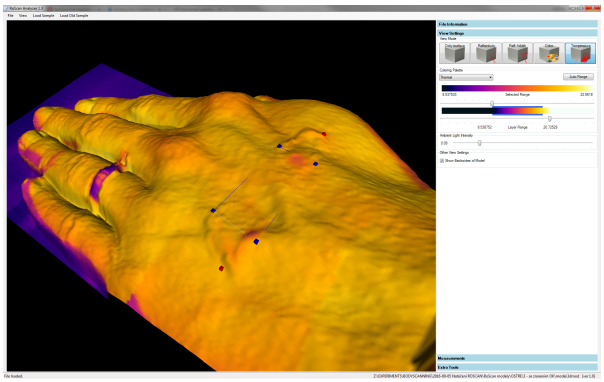

Fig. 4.10: Detail of 3D model of hand in the thermal coloured surface view, rebutting the presumption of burn.

Each model can be viewed in coloured view, thermal view, roughness view and surface only view. The colour layer provides possibility of precise selection of ROI according to markers drawn on the subject's skin. The thermal layer helps find the inflamed areas or determine if the spatial change is caused by physiological or non-physiological processes. And finally 3D scanning brings undistorted view, which is common for standard 2D imaging technologies and which disqualify the possibility of objective measurements.

In Fig. 4.9, the patient with presumed burn of hand is shown. The selection markers had been placed for further examination of temperature. In Fig. 4.10, the same patient with presumed burn is shown. It is clear, that in the selected region (highlighted by markers) is no thermal gradient, what rebuts the presumption of burn. In this case, the subject is an actor pretending the burn and his hand injury is masked, what agrees with our assessments.

In each view mode, the measurement tool is active, allowing several values to be measured: distances, angles, surface area, volume, colour, roughness, temperature. For definition of ROI, two groups of selection markers are available.

The application allows export to standard formats (XYZ, PLY, PTS), but always at the expense of loss of information, since none of these formats can handle all the data together.

4.3 RoScan Key Parameters and Capabilities

Tab. 4.1: Key parameters of RoScan solution

Positional accuracy of model points Absolute position of point in the space (3 σ).	0.12 mm^2
Scanning speed Entire forearm is scanned in about 1 min.	10 mm/s
Scanning trajectory The trajectory can be set to be able to scan any part of the body.	flexible, programmable
Measured values Position means the surface model itself.	position, colour, temperature, roughness
Price of single model The only expenses are electricity costs.	approx 0.1 EUR
Price of device Acquisition costs of the solution.	approx 30 000 EUR
Export formats for other SW Model data can be exported as a mesh or point cloud.	PLY, PTS, XYZ

The key advantage of this solution is combination of spatial, colour and thermal data within single 3D model, bringing new research opportunities, which would not be realizable without it. It can be helpful for objective evaluation of spatial changes of body, e.g. monitoring of oedemas, muscle growth or muscle atrophy, but also for monitoring of inflammation or necrosis.

Declared accuracy, as same as performance of both calibration methods was carefully verified. Results can be found in the full text of thesis.

5 MEDICAL APPLICATIONS OF ROSCAN

RoScan is a multi-purpose 3D surface scanning solution, having possible utilization in many different applications in wide range from mechanical engineering to medicine. And just medicine is the area for which the device could be the most beneficial, since almost every injury, many diseases or pathological changes are characterized by local increase of temperature [26]. Such areas can be recognizable on thermal layer of RoScan and due to 3D representation, accurately measured without distortion, in the sense of evidence based medicine.

Based on the introduction (chapter 1) and state-of-the-art overview (chapter 2), some applications, that are potentially interesting for medicine, had been selected and pilot studies were performed. These studies are further presented in following text and their possible benefits for medicine are also discussed.

Fig. 5.1: Experimental setup or Roscan for its medical applications.

The pilot studies mentioned in this chapter are not the only ones that are potentially beneficial to medicine. There are also other domains of healthcare, where RoScan could provide the new objective data, bringing new evidences for decision-making in medical practice. We can name for example monitoring of necrotic tissue of subjects suffering with diabetes mellitus [27], evaluation of fat sustainability after lipografting intervention [28], or breast cancer and skin cancer research.

The studies regarding these applications have not only been completed until the end of authors PhD studies, but cooperation has been already set up with partner institutes and will be the subject of the future research.

5.1 Assessment of Dermatic Medicaments

For objective assessment of treatment efficacy performed by particular medicament, it is necessary to be able to objectively quantify the AD lesion during the time.

The best present methods for quantification of dermatitis requires experienced clinician or measures only in narrow selection (not in the whole tissue), what both can cause misinterpretations or bring uncertainties to output value.

RoScan is dealing with these disadvantages by using thermal imaging, which provides objective and straightforward value of surface temperature, which is not necessary to be interpreted by expert and reflects blood flow in entire affected tissue. Because RoScan incorporates also 3D scanning and colour camera, the thermal *quantification* is enabled. The ROI, which is marked on the skin of tested subject is clearly visible on the colour image. The average temperature of ROI can be computed from thermal data and because of 3D surface model, the information is not distorted.

In following text, the case study of monitoring inflammation related to eczema caused by an allergic reaction is presented. The inflammation development is studied using RoScan during eczema growth and after the application of two different external dermatologics.

This experiment shows new possibilities of dermatitis quantification and demonstrates advances beyond state of the art brought by RoScan.

5.1.1 Materials and Methods

The case study has been performed on subject suffering with allergy on hazel allergens. The experiment began when itchy and red lesions appeared on superior side of left forefoot, few hours after ingestion of small amount of allergic substance. The area of lesion had been highlighted by markers drawn on the skin and was divided into two parts, marked as V and K (Fig. 5.3).

During first stage of experiment, the subject was repeatedly scanned [1] using RoScan during 50 minutes period. After that, Protopic® 0.1% topical ointment was applied to the area K and ointment from shea butter and coconut oil was applied to the area V.

During second stage, the subject was once again repeatedly scanned using RoScan for following 31 hours. In first minutes, when reaction to dermatologics was expected, the spacing between measurements was 2-3 minutes, then approx. 15 minutes and then about 45 minutes. Most of measurements were taken during first 4 hours, when subject was present in the laboratory. At following 27 hours, only 3 measurement were taken due to unavailability of subject to come for measurements.

When processing the results, the areas K and V were selected on each thermal 3D scan using color layer of 3D surface model, where markings drawn on the skin of subject are visible. Average temperature and selected surface area of each region were then computed[2]. The area

[1] Exact time of scanning has been saved and used for further evaluation.

[2] Both values are directly provided by RoScan software tool

of selected ROI serves as controlling value, since it shall stay unchanged at all samples, even if captured from slightly different positions. The average temperature was used as quantitative parameter.

Because surface temperature of forefoot depends also on physical activity or ambient heating, reference temperature was measured on each scan. As a reference point, area of letter V marked on the skin was used. We are assuming, that external influences affect the entire surface equally.

For quantification of inflammation in affected area, following metric has been applied:

$$\delta_A(t) = \frac{\overline{T_A}(t) - T_R(t)}{\overline{T_A}(0) - T_R(0)} - 1 \tag{5.1}$$

where $\overline{T_A}(t)$ is average temperature of points belonging to the area A in time t, $T_R(t)$ is reference temperature in time t. In this context, the meaning of $\delta_A(t)$ is relative change of difference between area temperature and reference temperature, relatively to the time and state when dermatologics were applied[3]. Such relative metric had been chosen due to unequal distance of both areas from edge of body, what causes differences in absolute values of a temperature. This approach normalizes both values to the same scaled index and make both areas to be comparable between each other.

5.1.2 Experimental Results

Development of $\delta_K(t)$ and $\delta_V(t)$ during 31 hours after the application of ointments is shown on Fig. 5.2.

Temperature gradient in area treated by Protopic® 0.1% culminated at 45% gradient relatively to starting state, when area treated by ointment from shea butter and coconut oil culminated at 65%. From point of culmination, both areas are healing with similar trend.

Both areas were similarly progressing before application of drugs, as shown in Fig. 5.4. Note, that there is no significant difference between thermal progresses of both areas until application of ointments. After that, the characteristics become different.

In Fig. 5.5, there is a detail of first 100 minutes after application, which is not visible in full scale. The temperature of area K is growing faster than in area V, but after 10 minutes stops to grow and after that, the increase during the time is significantly slower.

5.1.3 Discussion

Both areas are evolving in similar way before application of dermatologics (Fig. 5.4), what might rebut the assumption, that both areas are affected by differently advanced inflammation and that both areas would be then evolving differently even if not treated. For further

[3]e.g. $\delta_A(1\,\text{min}) = 10\%$ means that during first 10 minutes after application, the gradient of area temperature relative to ref. point has grown by 10%

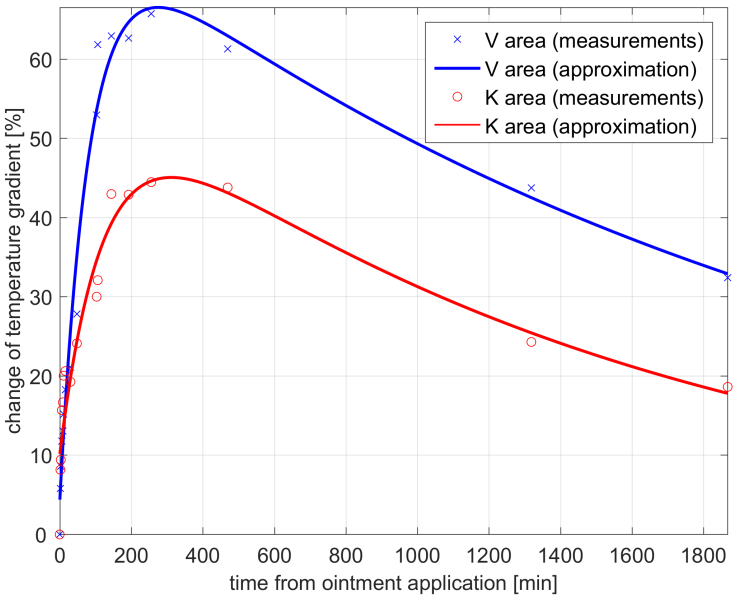

Fig. 5.2: Development of $\delta(t)$ during 31 hours after application of ointments.

Fig. 5.3: Affected area immediately after dermatologics application (top) and 31 hours later (bottom).

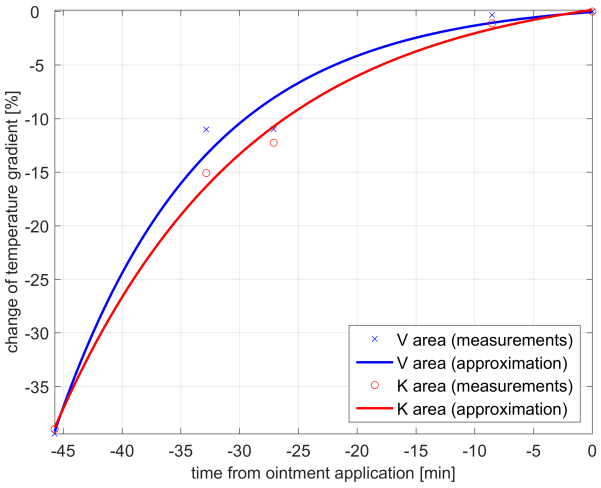

Fig. 5.4: Development of $\delta(t)$ before application of ointments.

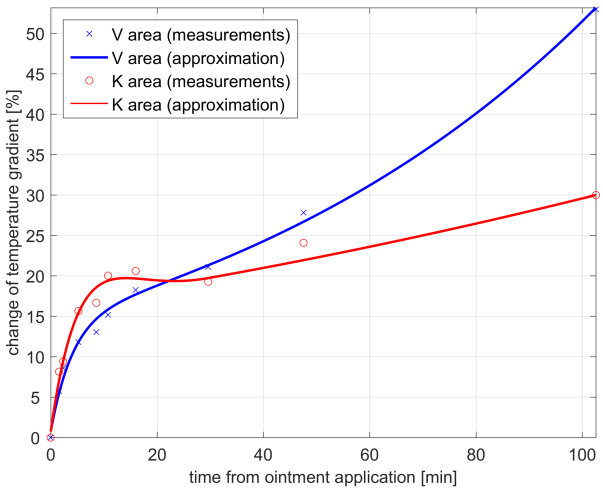

Fig. 5.5: Detail of $\delta(t)$ characteristics in first 100 minutes after application of ointments.

considerations, we assume that both areas are afflicted with inflammation of same severity, also because of the same symptoms (same redness, rash and itching).

Active substance of Protopic® 0.1% is Tacrolimus [29], what is topical calcineurin inhibitor (TCI), which works by weakening the skin's defense (immune) system, thereby decreasing the allergic reaction and relieving the eczema. Since atopic dermatitis is skin inflammation, which is partially caused by immunologic factors, its development should be reduced by dosing this drug.

On the contrary, the ointment from shea butter and coconut oil has no similar active substance and acts only as moisturizer for prevention from cracked skin.

This is in consensus with our observation from Fig. 5.2, where Protopic® 0.1% has stronger effect on stopping the development of eczema than ointment from shea butter and coconut oil.

According to subject's feelings, 2 minutes after application of ointments, the area K started to be strongly burning. This feeling culminated at 7 minutes and at 12 minutes burning in area K fully stopped, as same as previous itching. Itching in area V stays at same level during this period. The surface of area K also became sticky and oozing.

This report correlates with response of inflammation development in first minutes after drug application (Fig.5.5), where K area is initially more inflamed then V, but then inflammation decrease speed of development more than in area V. The burning after application is well known side effect of Protopic® 0.1% [29], but its cause is not known. Anyway, it is recognizable on time evolution of 3D thermogram.

5.1.4 Advances Beyond State of the Art

The main purpose of RoScan is being able to quantify inflammatory processes inside the human body. Case study above shown, that using RoScan for quantifying inflammation is possible.

Compared to methods used in everyday clinical practice (scoring systems), RoScan is more objective and especially disposes with significantly higher resolution. Used scoring systems are mostly based on visual observations [27] and when looking at differences between Fig. 5.3 left and right, it is clear, that RoScan brings more evidence-based diagnostic data.

However, even if we compare RoScan with objective bioengineering methods used in research and medicament trials (section 2.4), the several advances have been reached. At first, the interpretation is straightforward and experienced clinician is not necessary as for evaluating OCT, HFUS or RCM. Thus, the chance of misinterpretation is eliminated. At second, exactly the area of lesion is examined, not including the surroundings as in FDI and not just selected cross-sections as in OCT, HFUS and RCM.

It is important to say, that this experiment would not be realizable at all with any present method from state of the art. Current clinical trials are usually performed by two groups of subject, when one group is treated with the tested medicament and second is not, what may lead to wrong conclusions, when the selection group is not a representative sample of the population. Also the sensitivity of that methods are lower, so only significant progress is distinguishable.

RoScan allows comparing effects of two drugs *on the same subject* and even *on the same lesion*, what would not be possible by current methods. Due to its sensitivity and selectivity, it is also possible to evaluate the progress of treatment in significantly more detail, what was shown in this study in Fig. 5.4.

Last but not least advantage of RoScan is availability of more quantitative parameters in same time, when current methods are focused usually at single one. Besides lesion tem-

perature, also its colour, reflectance, roughness parameters of lesion surface and its area are available.

5.2 Volumetric Measurements of Soft Tissues

There are several commonly used methods, but there is a lack of clear comparison, which shows their advantages and limits. The accuracy of each method available is only roughly and uncertainly estimated in current publications. As a result of this, the validation study of Frustum Sign Method (FSM), Disc Model (DM), Partial Frustum Model (PFM), Water Displacement (WD), MRI and CT had been performed by author of this thesis and published in impacted journal [4]. The study is focused on accuracy and repeatability of each method.

These results were than compared also with RoScan, what demonstrates advances beyond state of the art brought by RoScan in the field of medical volumetric measurements.

RoScan, regarding its parameters and capabilities (section 4.3), brings faster, safe and more accurate solution with very low operational costs. It is especially valuable in specific cases, where advanced ROI examination is necessary.

5.2.1 Materials and Methods

Both comparative experiments are briefly described: accuracy and repeatability verification experiment and personal dependency test. The procedures taken for particular methods are described in the full text of thesis only.

Reference Objects

For verification of accuracy of Water Displacement Method and the circumferential measurements, we use precise aluminium cylinders in three sizes (Fig. 5.6 left) with volumes similar to finger, hand and forearm. Dimensions of each reference cylinder has been measured with slide calliper and according to [30], their volumes and uncertainties were computed.

For verification of accuracy of Magnetic Resonance Imaging and Computed Tomography, as same as for comparative experiments among different methods, two real human limbs were used. At subject's limb, borders of three regions of interest were marked with permanent marker (Fig. 5.6 right).

Accuracy and Repeatability Experiments

Since there is no universal object, which volume can be exactly computed and at the same time it is measurable by all compared methods, the experiments were processed as follows:

First step The accuracy of Water Displacement and all three circumferential methods has been verified on precise reference cylinders with known volume. Each cylinder was measured using each method 10 times (by the same person) in order to determine its repeatability.

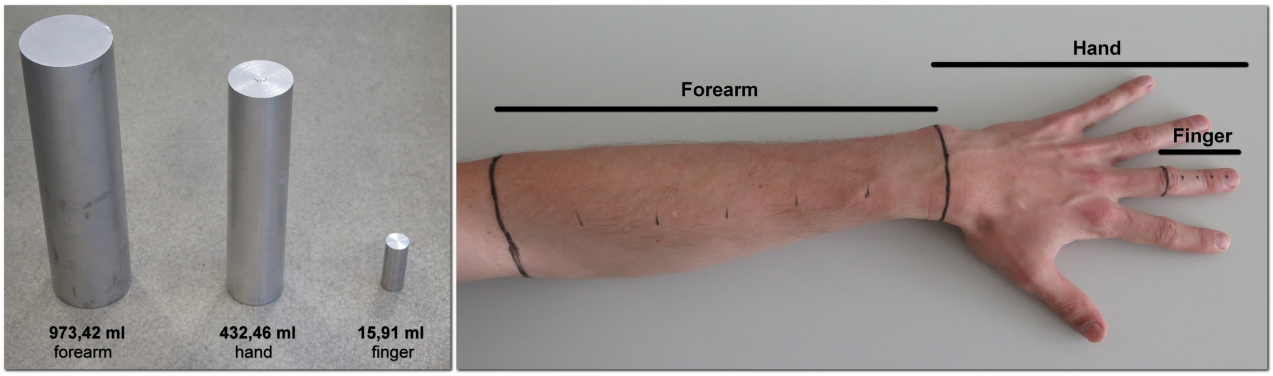

Fig. 5.6: Precise reference cylinders for verification of accuracy of Water Displacement Method and circumferential methods (left) and subject's upper limb with marked region of interest – Forearm, Hand and Finger regions.

Second step All the methods were tested on the patients. Two subjects, 26 and 39 years old, currently without pathological findings, were used for measurements of Forearm, Hand and Finger regions. Measurement of each region on every patient was also performed 10 times. Results of this step are shown in Figure 5.8.

Since aluminium objects are not allowed for CT and MRI, it was not possible to verify accuracy of CT and MRI on reference object. For the sake of evaluation, as reference values for assessment of CT and MRI accuracy, the value provided by Water Displacement method was taken, as long as it is considered as standard golden method.

Accuracy Relative absolute accuracy (RACC) was computed as relative difference between measured value of volume and true value of volume.

Repeatability Relative standard deviation (RSD) was computed as standard deviation of measured values in case of same object and same person performing the measurement.

Personal Dependency Test

In case of circumferential measurements, the result value of volume is dependent on particular person performing the measurement, since the value affects how much the string is tightened.

Three sets of 10 measurements on the same Forearm region using each circumferential method were performed by three different people in order to test personal dependency of the method.

5.2.2 Experimental Results

Diagrams in Fig. 5.7 and 5.8 show median, first and third quartile, minimal and maximal measured value for each method.

In comparison of methods with reference cylinders of known volume (Fig. 5.7), only RoScan and WD were close to true value. RoScan has significantly better repeatability on bigger volumes and its measured value is also slightly closer to true value compared to WD. Other methods overestimated or underestimated the value, what is given by their approximating principle.

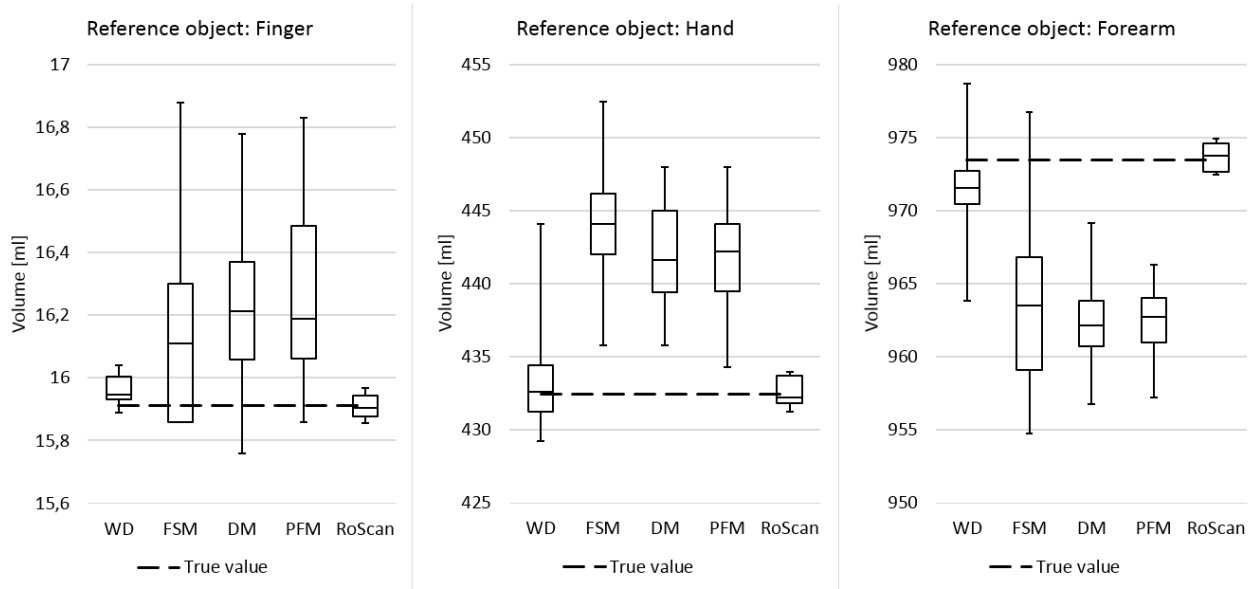

Fig. 5.7: Results of comparison among circumferential methods and Water Displacement method performed on reference object with known volume.

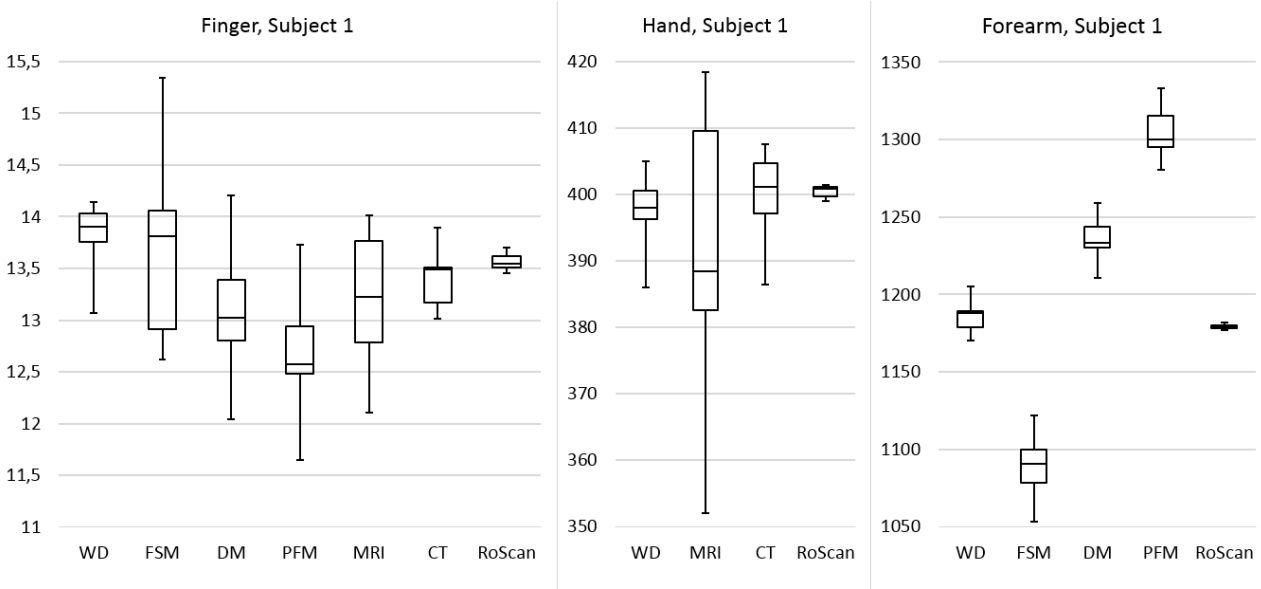

Fig. 5.8: Results of comparison among tested methods performed on subject 1.

In inter-method comparison (Fig. 5.8), the very strong correlation between CT and RoScan values was observed. Correlation between WD and RoScan was observed too. Other methods

were overestimating or underestimating again. The repeatability was strongly the best at RoScan in all cases. The second best was WD.

5.2.3 Discussion

The RoScan has been found as a method with the best repeatability (RSD up to 0.5 %) and also the accuracy (RACC = 0.05 %) in all tested experiments. It was also very fast (1 min. scanning and up to 10 min. processing), comparable even to the fastest, but the least accurate FSM method.

From current methods, the Water Displacement method can be considered as the best, since it has very good accuracy (RACC = 0.3 %) and repeatability (RSD up to 2 %). It is also very simple and it is observer independent.

The Frustum Sign Model was very fast (less than 1 min.), but it was very personally dependent in both accuracy and repeatability. The repeatability was in range from 2% to 6% and accuracy in range from 2 % to 8 % according the observer. But difference in resulting value in case of measurements of the same object by various observers was up to 10 %. On the other side, the best single observer was able to measure with RACC = 1.8 % and RSD = 1.5 %.

Both Disc Model and Partial Frustum Model were also personally dependent, but the repeatability was better (1 – 2 % Forearm, 3 – 4 % Finger). The best observers reach also better accuracy (up to 1 %).

The MRI and CT based measurements were significantly more expensive, but there are the only methods, where selecting of special region is allowed. Since MRI has lower resolution and there is also more noise in MRI data, the edge of object is harder to detect precisely, so the repeatability was lower in case of MRI (5 %) compared to CT (2 %). Also the accuracy was very good in case of CT (2 % Finger, 0.5 % Hand). The CT is the only one from current methods, which reaches up to the same accuracy and repeatability as the Water Displacement Method; however its use has adverse effect on human health.

5.2.4 Conclusion

According to [31] or [32], the WD method is considered as currently the best method based on its repeatability. This experiment is conform to this claim and besides reliability, it evaluates also accuracy related to the true value, what is also the best from current methods (Fig. 5.7).

This experiment also confirmed repeatability of FSM and DM given in [33] and evaluated accuracy, which is worse than WD's. On the other hand, this method cannot be considered as useless, since it is much faster than WD. It depends, how accurate measurement is necessary, but in some cases, its accuracy can be sufficient.

Modifications of FSM, DM and PFM, which were originally introduced in order to improve the accuracy. This experimental study examined, that improvement of accuracy is insignificant, especially in contrast with increase of measure time.

The experiment also proved and quantified the assumption of [34] that measured value is dependent on skills of person performing measurement.

For cases, when advancer selection of ROI is necessary, the RoScan, CT or MRI must be used, even though these methods are not as simple in equipment as previous ones.

The RoScan is very fast and easy to use and disposes with the best repeatability and accuracy from all methods ever. It is the best method in cases, when advanced ROI around surface is necessary, or in cases of detection of very tiny volumetric changes. It can be considered as the most advanced method, however the equipment needed (the RoScan 3D scanner itself) is quite expensive. On the other hand, it is still significantly less expensive than CT or MRI and its operation is inexpensive, what is not in cases of CT or MRI.

When ROI selection around inner structures is necessary, the MRI or CT are the only way, even when these methods are very time consuming, expensive, and with limited availability.

5.2.5 Advances Beyond State of the Art

Contribution to general knowledge is already a comparison of current methods itself as this has not been done yet, and the precision and repeatability parameters of current standard methods were only unreliable estimations until issuing of this paper.

But the experiment principally proved, that RoScan scanning system can be used as valid volumetric method, which is even better than current golden standard, Water Displacement method. Besides better accuracy and repeatability, the volumetric measurement is also faster than WD and allows selection of advanced ROI according to markers, which can be simply drawn on patient's skin.

It should be emphasized, that advanced ROI selection is a significant advantage over the current methods as this need can be currently solved only by MRI or CT, what are very slow, cumbersome and expensive methods. Due to their expensiveness, the availability is very limited[4], what makes repeated monitoring on day basis impossible.

Development of RoScan made this now possible, bringing new advanced and objective method, allowing for example comparative study of several exercises in rehabilitation, monitoring of muscle strengthening or atrophy in detailed scale, assessing the impact of therapy, etc. And due to the best accuracy, even tiny changes of volume can be distinguished.

Another important advantage of this method is, that also the purpose of volumetric change can be determined in some cases. Thermal data layer could help e.g. to discriminate between edema and positive influence of muscle strengthening.

Author is aware of the fact, that acquisition costs of RoScan are not negligible, but it is still 20 times lower than MRI [35] and 4 times lower than CT [36]. Beside this, RoScan operational costs are minimal and this device is not a single-purpose and can be used in many other medical sectors.

[4]For example in CZE, there is only 17 CT devices and 8 MRI devices per 1 million of inhabitants.

6 CONCLUSIONS

The output of the research connected with this thesis is a multispectral 3D surface scanning system RoScan, usable in many different sectors ranging from purely technical applications to specific medical applications. This system is based on the novel scanning method developed by author, which has not been available before, and which is using robotic manipulator and several sensors mounted on its end-point.

This approach enables reaching both *high flexibility* of scanning and *high absolute accuracy* of resulting 3D model in the same time, what is not common in current commercial 3D scanners, which are usually dealing with compromise between accuracy and flexibility. Beside this, it is also able to create *extensive* 3D models with keeping the high accuracy, what is also not common in current state of the art.

These extensive high-accurate models are covered with thermal data, which can have *the same resolution* as the high-accurate 3D surface model itself, what is moving forward the state of the art in the 3D Medical Thermal Imaging. In this domain, several experimental prototypes of 3D thermographic devices were published, but all of them disposed with many times lower resolution of thermal layer than 3D model itself, what was limiting its clinical usability. RoScan successfully deals with this issue by capturing more thermal frames from a smaller distance, what enables achieving the same resolution as other sensors. Note, that this would not be possible using different method.

RoScan has been validated in pilot studies in dermatology and physiotherapy. In both medical sectors brings advances beyond state of the art, what was demonstrated by clinical experiments.

In dermatology, RoScan has been used for monitoring eczematic lesion of subject suffering from atopic dermatitis. Its reaction to two different medicaments was successfully quantified *on the same subject in the same time*, what is not possible with current methods. This contributes to solve the common problem in comparative studies, when dermatitis in both tested groups can be evolving differently, what can lead to distorted results, or even to wrong conclusions. This method allows to test e.g. several ointments on not only single subject, but also on *single lesion*, what eliminates this issue.

Quantification of dermatitis by RoScan brings also higher sensitivity and selectivity compare to the current state of the art, as same as availability of more other quantitative parameters during the evaluation.

In physiotherapy, the current issue in quantification of limb volume is a lack of accurate, but fast method, which allows measurements of specific region of interest (ROI). It forces clinicians and researchers to use in such cases CT or MRI, what both are methods intended for another purposes and having many important disadvantages and limitations.

Introducing RoScan brings new volumetric method, which is dealing with this issue. Among possibility of ROI, it moves the current state of the art forward also by the best repeatability and accuracy among all currently available methods.

Beside this, RoScan models brings also ability to preserve the exact condition of the patient's body (for comparison during the next visit at the clinician), what allows to objectively evaluate the progress of disease, even if changes are very small; or possibility to assess, if spatial changes of body are caused by physiological (e.g. muscle growth) or non-physiological factors (e.g. edema).

Dermatology and physiotherapy are not the only sectors, when RoScan can be useful. We can name for example monitoring of necrotic tissue of subjects suffering with diabetes mellitus [27], evaluation of fat sustainability after lipografting intervention [28], or breast cancer and skin cancer research.

Cooperation has been already established with clinical partners from St. Anne's University Hospital Brno (FNUSA), The Univerity Hospital Brno (FN brno) and The Children Hospital (Detska nemocnice FN Brno) in clinics of dermatovenereology, plastic surgery, diabetology and burns and reconstructive surgery, who are interested in this method. With these partners, new clinical applications of RoScan will be searched and tested in further work.

The method will be also further continuously developed and improved within the H2020 project ASTONISH funded by the European Union ECSEL framework, in which the RoScan has been included as one of its 6 main Use-Cases. The project is focused on novel devices, bringing reduction of hospitalization time and shortening the patient's recovery time. There are 24 institutions from 6 countries involved in ASTONISH.

AUTHOR PUBLICATIONS

Papers [1, 2, 3, 4, 5, 6, 7, 8, 9, 10] are author's original works publishing results summarized above. Publications [4, 7] are impacted journals, publications [2, 3, 6] are SCOPUS journals and publications [1, 5, 8, 9, 10] are conference papers.

Publications [1, 2, 3, 6, 7, 10] are dealing with issues related to development of robotic 3D scanning system and publications [4, 5, 8, 9] are devoted to its medical applications.

In all these publications, the author of this thesis is the main corresponding author.

BIBLIOGRAPHY

[1] Adam Chromy, Petra Kocmanova, and Ludek Zalud. Creating Three-Dimensional computer models using robotic manipulator and laser scanners. In *12th IFAC Conference on Programmable Devices and Embedded Systems (2013)*, Programmable devices and systems, pages 268–273, Velke Karlovice, September 2013. Elsevier B.V.

[2] Adam Chromy and Ludek Zalud. Novel 3D modelling system capturing objects with Sub-Millimetre resolution. *Advances in Electrical and Electronic Engineering*, 12(5):476–487, December 2014.

[3] Adam Chromy and Ludek Zalud. Robotic 3D scanner as an alternative to standard modalities of medical imaging. *SpringerPlus*, 3(1):13, 2014.

[4] Adam Chromy, Ludek Zalud, Petr Dobsak, Igor Suskevic, and Veronika Mrkvicova. Limb volume measurements: comparison of accuracy and decisive parameters of the most used present methods. *SpringerPlus*, 4(1):707, November 2015.

[5] Adam Chromy. High-Accuracy volumetric measurements of soft tissues using robotic 3D scanner. *IFAC-PapersOnLine*, 48(4):318–323, January 2015.

[6] Adam Chromy. Application of High-Resolution 3D scanning in medical volumetry. *International Journal of Electronics and Telecommunications*, 62(1):23–31, March 2016.

[7] Adam Chromy and Ondrej Klima. A 3D scan model and thermal image data fusion algorithms for 3D thermography in medicine. *Journal of Healthcare Engineering*, 2017. In press.

[8] Adam Chromy and Ludek Zalud. Three-dimensional thermal imaging in medicine. In *3DBODY.TECH 2017 - 8th International Conference and Exhibition on 3D Body Scanning and Processing Technologies*, pages 232–238, Montreal, Canada, October 2017. Hometrica Consulting - Dr. Nicola D'Apuzzo.

[9] Adam Chromy. Multispectral 3D surface scanning system RoScan and its application in inflammation monitoring and quantification. Manuscript submtted for publication., 2017.

[10] Adam Chromy. Mutual calibration of sensors for multispectral 3D scanning of surface. In *The 9th International Congress on Ultra Modern Telecommunications and Control Systems*, Munich, 2017. Manuscript accepted for publication.

[11] Valerie C. Coffey. Multispectral imaging moves into the mainstream. *Optics and Photonics News*, 23(4):18–24, April 2012.

[12] J.H. Park. Digital restoration of seokguram grotto: The digital archiving and the exhibition of south korea's representative UNESCO world heritage. In *Proceedings of 2012 International Symposium on Ubiquitous Virtual Reality, ISUVR 2012*, pages 26–29, 2012.

[13] S. Klein, M. Avery, G. Adams, S. Pollard, and S. Simske. From scan to print: 3D printing as a means for replication. *HP Laboratories Technical Report*, 2014.

[14] Ricardo Vardasca and Ricardo Simoes. Current issues in medical thermography. In *Topics in Medical Image Processing and Computational Vision*, Lecture Notes in Computational Vision and Biomechanics, pages 223–237. Springer, Dordrecht, 2013. DOI: 10.1007/978-94-007-0726-9_12.

[15] Brian Curless. From range scans to 3D models. *SIGGRAPH Comput. Graph.*, 33(4):38–41, November 1999.

[16] Jeanne Duus Johansen, Peter J. Frosch, and Jean-Pierre Lepoittevin. *Contact Dermatitis*. Springer Science & Business Media, September 2010. Google-Books-ID: sSHIlWSOiroC.

[17] Francesco Lacarrubba, Giovanni Pellacani, Silvia Gurgone, Anna Elisa Verzì, and Giuseppe Micali. Advances in non-invasive techniques as aids to the diagnosis and monitoring of therapeutic response in plaque psoriasis: a review. *International Journal of Dermatology*, 54(6):626–634, June 2015.

[18] Min-Bin Chen. A parallel 3D delaunay triangulation method. In *2011 IEEE 9th International Symposium on Parallel and Distributed Processing with Applications (ISPA)*, pages 52–56, May 2011.

[19] Mark de Berg, Marc van Krevel, and Mark Overmars. *Computational geometry: algorithms and applications*. Springer, Berlin, 3rd ed edition, 2008.

[20] Kevin Suffern. *Ray Tracing from the Ground Up*. CRC Press, March 2016.

[21] Tomas Möller and Ben Trumbore. Fast, minimum storage Ray/Triangle intersection. In *ACM SIGGRAPH 2005 Courses*, SIGGRAPH '05, New York, NY, USA, 2005. ACM.

[22] T. L. Kunii. *Frontiers in Computer Graphics: Proceedings of Computer Graphics Tokyo '84*. Springer Science & Business Media, December 2012. Google-Books-ID: YYyrCAAAQBAJ.

[23] Simon Josefsson. The base16, base32, and base64 data encodings. tools.ietf.org/html/rfc4648, 2006.

[24] J. Canny. A computational approach to edge detection. *IEEE Transactions on Pattern Analysis and Machine Intelligence*, PAMI-8(6):679–698, November 1986.

[25] Jean-Yves Bouquet. Camera calibration toolbox for matlab, 2015.

[26] Tien-Chun Chang, Yung-Lien Hsiao, and Shu-Lang Liao. Application of digital infrared thermal imaging in determining inflammatory state and follow-up effect of methylprednisolone pulse therapy in patients with graves' ophthalmopathy. *Graefe's Archive for Clinical and Experimental Ophthalmology*, 246(1):45–49, January 2008.

[27] Dmitri V. Krysko, Tom Vanden Berghe, Katharina D'Herde, and Peter Vandenabeele. Apoptosis and necrosis: detection, discrimination and phagocytosis. *Methods (San Diego, Calif.)*, 44(3):205–221, March 2008. PMID: 18314051.

[28] Thomas L. Tzikas. Lipografting: autologous fat grafting for total facial rejuvenation. *Facial plastic surgery: FPS*, 20(2):135–143, May 2004. PMID: 15643580.

[29] Melissa C. Lazarous and Francisco A. Kerdel. Topical tacrolimus protopic. *Drugs of Today (Barcelona, Spain: 1998)*, 38(1):7–15, January 2002. PMID: 12532181.

[30] Thomas Jamerson. Uncertainty example using simple propagation of uncertainty rules, August 2009.

[31] A. M. Megens, S. R. Harris, C. Kim-Sing, and D. C. McKenzie. Measurement of upper extremity volume in women after axillary dissection for breast cancer. *Archives of Physical Medicine and Rehabilitation*, 82(12):1639–1644, December 2001. PMID: 11733875.

[32] D. M. Kaulesar Sukul, P. T. den Hoed, E. J. Johannes, R. van Dolder, and E. Benda. Direct and indirect methods for the quantification of leg volume: comparison between water displacement volumetry, the disk model method and the frustum sign model method, using the correlation coefficient and the limits of agreement. *Journal of Biomedical Engineering*, 15(6):477–480, November 1993. PMID: 8277752.

[33] T. Deltombe, J. Jamart, S. Recloux, C. Legrand, N. Vandenbroeck, S. Theys, and P. Hanson. Reliability and limits of agreement of circumferential, water displacement, and optoelectronic volumetry in the measurement of upper limb lymphedema. *Lymphology*, 40(1):26–34, March 2007. PMID: 17539462.

[34] J. M. Armer and S. H. Ridner. Measurement techniques in assessment of lymphedema. *Lymph Link Article Reprint*, 18(3):1–4, September 2006.

[35] Magnetic resonance imaging. http://www.mri-portal.com/clanky/magneticka_rezonance.php, 2010.

[36] C. H. McCollough and F. E. Zink. Performance evaluation of a multi-slice CT system. *Medical Physics*, 26(11):2223–2230, November 1999. PMID: 10587202.

ABSTRACT

Both Thermal Imaging and 3D Scanning are currently rapidly progressing technologies. Both technologies has many advantages, which could be useful in medicine. Merging them together brings even more new diagnostic information, than if used separately. The aim of this thesis is development of multispectral 3D surface scanning system based on novel scanning method, using robotic manipulator equipped with laser scanner, thermal camera and colour camera. Such solution bring both flexibility and accuracy. This scanning system is further used in clinical applications in order to verify its abilities and demonstrate its advances beyond state of the art.

KEYWORDS

Multispectral 3D Scanning; Medical Quantification; Robotic 3D Scanning; Quantification of Dermatitis; Medical Volumetry.

ABSTRAKT

Termovizní zobrazování i 3D skenování jsou v současné době rychle se rozvíjející technologie. Obě technologie mají mnoho výhod, které by mohly být užitečné v medicíně. Jejich datová fúze přináší ještě více nových diagnostických informací, než kdyby byly použity samostatně. Cílem této práce je vývoj multispektrálního 3D skenovacího systému založeného na novém způsobu snímání pomocí robotického manipulátoru vybaveného laserovým snímačem, teplotní kamerou a barevnou kamerou. Navržené řešení přináší jak flexibilitu, tak přesnost. Tento systém skenování je dále využit v klinických aplikacích, aby byly ověřeny jeho schopnosti a ukázany přínosy nad rámec současného stavu techniky.

KLÍČOVÁ SLOVA

Multispektrální 3D skenování; Kvantifikace v medicíně; Robotické skenování; Kvantifikace dermatitidy; Medicínská volumetrie.

CHROMÝ, Adam. *High-Resolution Multispectral 3D Scanning and its Medical Applications*. Brno, 2017, 32 p. Doctoral thesis. Brno University of Technology, Faculty of Electrical Engineering and Communication, Department of Control and Instrumentation. Advised by prof. Ing. Luděk Žalud, Ph.D.